

AD-A125 831

PROCESSING OF DIGITAL IONOGRAMS(U) LOWELL UNIV RESEARCH 1/1
FOUNDATION MA B W REINISCH APR 81 ULRF-414/CAR
AFGL-TR-81-0085 F19628-88-C-0064

UNCLASSIFIED

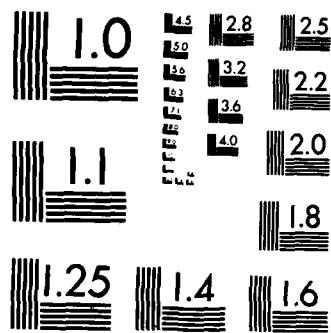
F/G 9/2

NL



END

19628



MICROCOPY RESOLUTION TEST CHART
NATIONAL BUREAU OF STANDARDS-1963-A

ADA125831

AFGL-TR-81-0085

(D)

PROCESSING OF DIGITAL IONOGRAMS

Bodo W. Reinisch

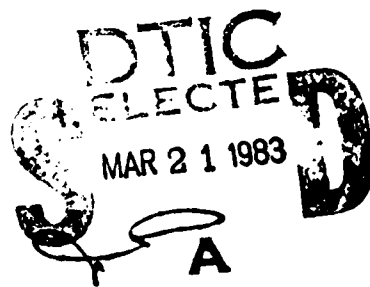
University of Lowell
Center for Atmospheric Research
450 Aiken Street
Lowell, Massachusetts 01854

Scientific Report No. 1

April 1981

Approved for public release; distribution unlimited.

AIR FORCE GEOPHYSICS LABORATORY
AIR FORCE SYSTEMS COMMAND
UNITED STATES AIR FORCE
HANSCOM AFB, MASSACHUSETTS 01731



DTIC FILE COPY

83 03 21 020

**Qualified requestors may obtain additional copies from the
Defense Technical Information Center. All others should
apply to the National Technical Information Service.**

UNCLASSIFIED

SECURITY CLASSIFICATION OF THIS PAGE (When Data Entered)

UNCLASSIFIED

SECURITY CLASSIFICATION OF THIS PAGE(When Data Entered)

20. Abstract

on some 1000 ionograms with good success.

A simple microcomputer algorithm is shown which calculated the electron density profiles from the $h'(f)$ trace during the 1978 Kwajalein Equatorial Spread F campaign.

↑

UNCLASSIFIED

SECURITY CLASSIFICATION OF THIS PAGE(When Data Entered)

TABLE OF CONTENTS

	Page
1.0 INTRODUCTION	1
2.0 AUTOMATIC SCALING OF IONOGRAMS	2
3.0 AUTOMATIC PARAMETER EVALUATION	4
4.0 REAL TIME ELECTRON DENSITY PROFILES	6
5.0 DOPPLER IONOGRAMS	9
6.0 REMOTE TRANSFER OF DIGITAL IONOGRAMS IN REAL TIME	11
SUMMARY	13
ACKNOWLEDGEMENT	14
REFERENCES	15



Acceptation No. 5

NTIS	CR/31
111-1007	111-1007
Univ. of Texas	Univ. of Texas
7	7

X

A

LIST OF FIGURES

Figure No.		Page
1	AUTOMATIC IONOGRAM SCALING	16
2	IONOSPHERIC CHARACTERISTICS	17
3	EXAMPLE OF IONOGRAM TO SHOW THE Z COMPONENT EXAMPLE TO SHOW THE ERROR IN A.P.E. IN DETERMINING f_{oF2}	18
4	DIURNAL VARIATION OF ERROR (MANUAL f_{oF2} - A.P.E. f_{oF2}) 948 IONOGRAMS 5-13 JANUARY 1979 GOOSE BAY, LABRADOR	19
5	DIURNAL VARIATION OF ERROR [MANUAL $MUF(3000)$ -A.P.E. $MUF(3000)$]/MANUAL $MUF(3000)$] 938 IONOGRAMS 5-13 JANUARY 1979 GOOSE BAY, LABRADOR	20
6	OBLIQUE IONOGRAMS	21
7	AIRCRAFT IONOSONDE-THULE 09 DEC 1979 2214 (UT)	22
8	DIRECTIONAL IONOGRAMS WITH DOPPLER	23
9	GOOSE BAY IONOSPHERIC OBSERVATORY 26 JUL 1979 04:39 AST	24

1.0 INTRODUCTION

— This presentation is a summary of digital ionogram processing techniques developed by ULCAR in the recent past. Real-time and on-line methods were emphasized and this implies continuing improvement and increasing complexity of the processing algorithms along with the technological advancements. Of course, a mini or mainframe computer with sufficient memory could perform the processing described here. But for on-line operation at an ionosonde field site cost and environmental conditions generally exclude this approach, and special purpose hardware/microprocessor techniques are the only adequate method. The difference between mini- and microcomputers is diminishing, but the modular microcomputer systems have the advantage of being easily integrated into a digital ionosonde at low costs. The Digisonde 128PS (Bibl and Reinisch, 1978a; 1978b) initially outputs complete ionograms (in the ionogram mode) with amplitude, phase, doppler, incidence angle and/or polarization for each frequency-range bin. Post-processing of these ionograms can then extract the ionospheric parameters required for specific investigations.

2.0 AUTOMATIC SCALING OF IONOGRAMS

The initial ionogram contains a large amount of information of which not all is necessarily required for synoptic studies or investigations interested only in specific parameters. In such cases it may suffice to "scale" the ionogram by automatically determining the heights and amplitudes of the main echo traces. For undisturbed ionograms the task is relatively simple as long as the distinction between ordinary and extraordinary echoes does not become too difficult. Figure 1 shows the result of a simple algorithm that was applied to a mid-latitude ionogram. This algorithm, implemented in the Geomonitor (Reinisch and Smith, 1976) that is connected to the Digisonde at AFGL's Goose Bay Ionospheric Observatory, Labrador (Buchau et al, 1978) and in the Automatic Ionogram Collator at the U.S. Army Digisonde in Fort Monmouth, New Jersey, extracts amplitude, height and spread of the echoes from the ionogram. These collated data can be presented in the frame of an ionogram to verify the accuracy of the algorithm, as shown on top of Figure 1, or they can be printed in the form of ionospheric characteristics. Figure 2 shows E and F echo amplitudes as function of frequency and time (panels 2, 3, 4 and 5), and the range for backscatter observations (panel 1) as function of time for a period of six days in Goose Bay. Each vertical line contains the data of one ionogram. The envelopes of the amplitude-versus-frequency characteristic give essentially the diurnal variations of the critical frequencies for E and F-region. Disturbed ionospheric conditions, like on days 291/292 1977 are easily recognizable.

Most ionograms are, of course, not as simple as the one shown for a mid-latitude station in Figure 1. Figure 3 shows two somewhat more complicated ionograms from AFGL's Goose Bay Ionospheric Observatory and the "echo" points detected by the on-line Geomonitor. Of special interest is

the upper ionogram from 10 January 1979 which contains a strong Z-trace. Now, even though the new Digisonde 128PS tags each frequency-range bin with an O or X-flag the Z-trace is not distinguished from the O-trace since both have the same polarization. Since the Geomonitor detects up to six frequencies for each sounding frequency it will pick up both the O and the Z-trace and the Automatic Parameter Evaluation (A.P.E.) program (Section 3.0) will determine a false foF2. In general further processing is required to extract a unique trace that can serve as input to the true height algorithm. It is clear that a refined ionogram (or the corresponding profile) has lost information contained in the original ionogram, like oblique echoes and spread conditions. It is for that reason that for many investigations reliance on a few ionospheric parameters is dangerous, and the raw ionogram data must be preserved. On the other hand for routine monitoring of ionospheric conditions limitation to characteristic parameters becomes a necessity.

3.0 AUTOMATIC PARAMETER EVALUATION

Once the echo traces are determined it is possible to determine certain ionospheric parameters which in conventional systems are manually scaled. The Automatic Parameter Evaluation program (Smith et al, 1979) was applied to some 1000 Geomonitor processed Goose Bay ionograms to extract the parameters foF2, fmin, hmin, MUF(3000) and ftEs. For the period 5 to 13 January 1979 the automatically scaled values were compared with a data technician's visual interpretations. Figures 4 and 5 show the diurnal variations of the errors for foF2 and the MUF(3000). Considering that spread F occurrence and mid-latitude trough phenomena effected the majority of the ionograms during the 5 to 13 January period, the success rate shown in Figures 4 and 5 is fairly good during daytime and around local midnight. Performance during twilight times is unacceptably poor. The weak point in the automatic processing scheme is the presently used Geomonitor algorithm for the on-line echo trace detection under disturbed conditions. An improved algorithm applicable to both bottomside and topside ionograms (Reinisch et al, 1980) is presently being developed using the ionograms as an entity rather than making a frequency-by-frequency decision on what constitutes an echo. The recent advancements in memory technology allow on-line microprocessor implementation of this advanced algorithm.

Automatic determination of the predicted maximum usable frequency (MUF), for a given distance, from the vertical ionograms is not difficult for digital ionograms. Methods to determine MUF as function of time had been developed for analog sounders (Nakata et al, 1953; Bibl, 1956). Our digital algorithm (Smith et al, 1978) simply multiplies each frequency of the ionogram trace by the MUF factor calculated for a distance of 3000 km according to URSI specifications (Piggott and Rawer, 1972, p. 21) to generate the equivalent oblique

ionogram (Figure 6) from which the MUF can be scaled directly. More recently we applied this method to the raw ionograms rather than to the Geomonitor identified traces. The average error diminished because errors in the trace identifications no longer effects the MUF determination. Cormier and Dieter (1974) simulated the manual overlay technique with good success in a computer program to find the MUF. This method is, however, more susceptible to noise than the approach discussed above.

4.0 REAL TIME ELECTRON DENSITY PROFILES

For conversion of the $h'(f)$ ionogram trace into vertical electron density profiles the Digisonde contains a microcomputer program that performs the conversion in almost real time. The algorithm is based on the usual lamination technique for a monotonous profile assuming that $z(f_n)$, i.e. height as function of plasma frequency, is continuous and steady at slab transitions and that the second derivative of z with respect to f_N is constant within each slab (Paul, 1977; Bibl and Reinisch, 1978b, p. 98ff). This results in a recursive scheme that determines the height of plasma frequency f_n as:

$$z_n = z_{n-1} + D_{n-1} + \frac{1}{2} DD_{n-1}$$

$$D_{n-1} = (D_{n-2} + DD_{n-2}) \frac{f_n - f_{n-1}}{f_{n-1} - f_{n-2}}$$

$$DD_{n-1} = \frac{1}{S_{nn}} \{h'_n - z_0 - \sum_{i=1}^n D_{i-1} F_{ni} - \sum_{i=1}^{n-1} DD_{i-1} S_{ni}\}$$

$$F_{ni} = \frac{1}{f_i - f_{i-1}} \int_{f_{i-1}}^{f_i} \mu'(f, f_n) df$$

$$S_{ni} = \frac{1}{(f_i - f_{i-1})^2} \int_{f_{i-1}}^{f_i} \mu'(f, f_n) \cdot (f - f_{i-1}) df.$$

The group index of refraction $\mu'(f, f_n)$ is of course also a function of the gyrofrequency f_H . For the on-line profile calculations the coefficients F_{ni} and S_{ni} are tabulated for a given geomagnetic location and stored in PROM to achieve a fast profile conversion in the Microcomputer.

At the present time the ionogram-to-profile conversion is not fully automated. The f_n , h'_n data pairs must be

entered via keyboard. An example of the program input and output data is given in Table 1. These on-line electron density profiles are of great importance for special experiments like rocket campaigns. The example shown was made during a rocket/satellite/incoherent radar experiment in Kwajalein on 31 July 1978. The last column in the table shows the bottom-side scale length of the F-layer, giving the height interval within which the plasma frequency increases by 1 MHz. This scale height together with h_{minF} seems to control the spread F occurrence (Ossakow et al, 1978). No effort was made to refine the program with regard to the starting and valley problems. Instead we optimized for speed and ease of operation at the field site.

INPUT DATA, KW 78 0212 2300 LMT			TRUE HEIGHT PROFILE	
NR	FREQ. [100 kHz]	V. HEIGHT [KM]	Z [KM]	SCALE [KM/MHz]
00	00	313	313	
02	10	315	314	00
04	20	317	315	00
06	30	329	317	02
08	49	339	320	05
0A	50	350	328	10
0C	52	357	330	
0E	54	360	333	
10	56	364	335	
12	58	368	337	
14	60	370	339	30
16	62	385	342	
18	64	392	345	
1A	66	397	348	
1C	68	407	352	
1E	70	420	356	55
20	72	428	360	
22	74	439	364	
24	76	450	369	
26	78	455	373	
28	80	468	378	
2A	82	500	385	
2C	84	542	394	
2E	86	600	414	
300	FFFF			

ELECTRON DENSITY PROFILE
KWAJALEIN, 31 JULY 1978, 2300 LMT

TABLE 1

5.0 DOPPLER IONOGRAMS

The usefulness of multiparameter ionograms (Bibl and Reinisch, 1978a) is demonstrated by the ionograms recorded by AFGL's Airborne Ionosonde in Thule on 9 December 1979 (Figure 7). The amplitude ionograms in the lower right hand corner shows typical aurora region spread F conditions. The amplitude in each frequency-range bin is accompanied by a status word displayed in the upper right corner, forming a status ionogram. In this instance the status words represent signal doppler frequencies varying from -11 to +11 Hz. A simple microcomputer algorithm separated the original ionogram into two: one containing only echoes with negative doppler frequencies (upper left), and another with only positive doppler frequencies (lower left). In these doppler ionograms the amplitudes are replaced by doppler frequencies. The overhead ionosphere shows no significant motion, slightly positive and negative dopplers are observed. Predominantly negative doppler frequencies are observed for ranges between 400 and 600 km. The radial velocity of the reflecting ionization away from the sounder is 110 ms^{-1} . Between 8 and 9 MHz echoes with a strong positive doppler shift are seen at ranges between 600 and 700 km. The doppler frequencies indicate a radial velocity of the reflector of approximately 75 ms^{-1} .

If the status contains information on the incidence angle of the ionospheric echoes directional ionograms can reveal the structure of the local ionosphere. Figure 8 shows two directional ionograms from the 1978 Kwajalein equatorial spread F campaign. The receiving antenna array was scanning the vertical, northwest and southwest direction in the first ionogram, and vertical, northeast and southeast in the second one. The majority of the echoes come from overhead, even those echoes composing the range spread. All the vertical echoes have a positive doppler shift (dark numbers) indicating

a downward motion of the ionization. The echoes between 7 and 10 MHz from the northeast have predominantly negative doppler frequencies, the ionization is moving away. A sequence of directional and doppler ionograms is required to resolve the dynamical processes in the ionosphere.

6.0 REMOTE TRANSFER OF DIGITAL IONOGRAMS IN REAL TIME

Remote display of ionograms has become feasible with the advent of digital ionosondes. Transmission of digital ionograms via commercial telephone lines poses no major difficulties and allows to simultaneously monitor ionospheric conditions at the various locations of digital sounders. The need for real time remote ionogram information arises in a number of circumstances: monitoring the midpoint of high-frequency communication links or bistatic hf experiments, monitoring the ionospheric reflection points for over-the-horizon radar operation, or simply the testing of local field sites. The distances over which the transmission takes place may be less than 100 km in the latter case to more than 1000 km in the first examples. Simplex circuit telephone lines, or alternately microwave links, are sufficient for the ionogram transmission, even though half duplex circuits (or the use of reverse channels) are preferable since they allow handshaking procedures and data retransmission after error detection.

Figure 9 shows an ionogram from AFGL's Goose Bay Ionospheric Observatory, Canada, printed in Maine, U.S.A., approximately 1000 km south of Goose Bay (Smith et al, 1979). In the Centronics printer that was used for the generation of this ionogram the font-controlling ROM (read-only memory) was replaced by a differently programmed chip in order to produce the optical weighting of the number font. The time required for the remote transmission of an ionogram is given by the maximum baud rate of the modems and the telephone lines, and by the speed of the printer. Inexpensive modems and telephone lines limit the baud rate to 1200 bits per second, or 120 characters/sec. For an amplitude ionogram with 128 range bins (Bibl and Reinisch, 1978a) a little more than 1 sec is required for transmission of one data line. If the printer has a line buffer that accumulates the new line while printing

the previous one it takes less than three minutes for the remote printout of an ionogram with 160 frequencies (0 to 16 MHz in 100 kHz increments).

In general it is undesirable to impose the speed limitations of the remote printout facility onto the sounder operation. We therefore store a complete ionogram in memory and start remote transmission at the end of the ionogram scan. Some limited postprocessing was performed in the example shown in Figure 9: (1) signals with extraordinary polarization are suppressed, (2) all vertical echoes are underlined, (3) digital noise filtering is applied. Of course the specific type of postprocessing will depend on the user's requirements.

SUMMARY

Postprocessing of digital ionograms has become an important step of ionospheric research with ionosondes. The new digital ionosondes with their multiparameter data offer new opportunities for research and we have shown in a number of examples how automatic processing of the data can reveal specific ionospheric features.

ACKNOWLEDGEMENT

This work was in part sponsored by the U.S. Air Force under Contract No. F19628-78-C-0085 and by DNA under Contract No. DNA001-77-C-0187.

REFERENCES

"Simultaneous Measurement of Sweep Frequency $h't$ and fct of the ionosphere," Y. Nakata, M. Kan and H. Uyeda, Rep. on Ion. Res., Japan, 7, 129-135, 1953.

"Automatic Recording of Ionospheric Characteristics," K. Bibl, J.A.T.P., 8, 295, 1956.

"U.R.S.I. Handbook of Ionogram Interpretation and Reduction," Second Edition, ed. W. R. Piggott and K. Rawer, pub. World Data Center A, Boulder, Colorado, 1972.

"Automatic Processing of Digital Ionograms," R. Cormier and K. Dieter, AFCRL-TR-74-0502, 1974.

"Geomonitor - Digital Real Time Processor for Geophysical Data," B. W. Reinisch and S. Smith, AFGL-TR-76-0292, 1976.

"A Simplified Inversion Procedure for Calculating Electron Density Profiles from Ionograms for Use with Minicomputer," A. K. Paul, Radio Science, Vol. 12, No. 1, 119-122, 1977.

"Digisonde 128PS for Ionospheric Dynamics and Three-Dimensional Structure Studies," K. Bibl and B. W. Reinisch, pub. University of Lowell Center for Atmospheric Research, 1978a.

"The Universal Digital Ionosonde," K. Bibl and B. W. Reinisch, Radio Science, 13, 519-530, 1978b.

"Remote Ionospheric Monitoring," J. Buchau, W. N. Hall, B. W. Reinisch and S. Smith, Proceedings of the IES, paper 5-5, 1978.

"Remote Ionogram Communicator - ICOM," S. Smith, B. W. Reinisch, D. F. Kitrosser and K. Bibl, pub. University of Lowell Center for Atmospheric Research, 1979.

"Automatic Ionospheric Parameter Extraction from Digital Ionogram Data," S. Smith, B. W. Reinisch, J. S. Tang and K. Bibl, ULRF-404/CAR, 1979.

"Non-Linear Equatorial Spread F: Dependence on Altitude at the F-Peak and Bottomside Background Electron Density Gradient Scale Length," S. L. Ossakow, S. T. Zalesak, B. E. McDonald and P. K. Chatuovedi, J. Geophys. Res., 84, 17, 1979.

"Topside Ionogram Scaling Algorithm," B. W. Reinisch, H. Xueqin and J. S. Tang, Scientific Report No. 1, RCA Contract GX-FM9238-0601-00-F40, March 1980.

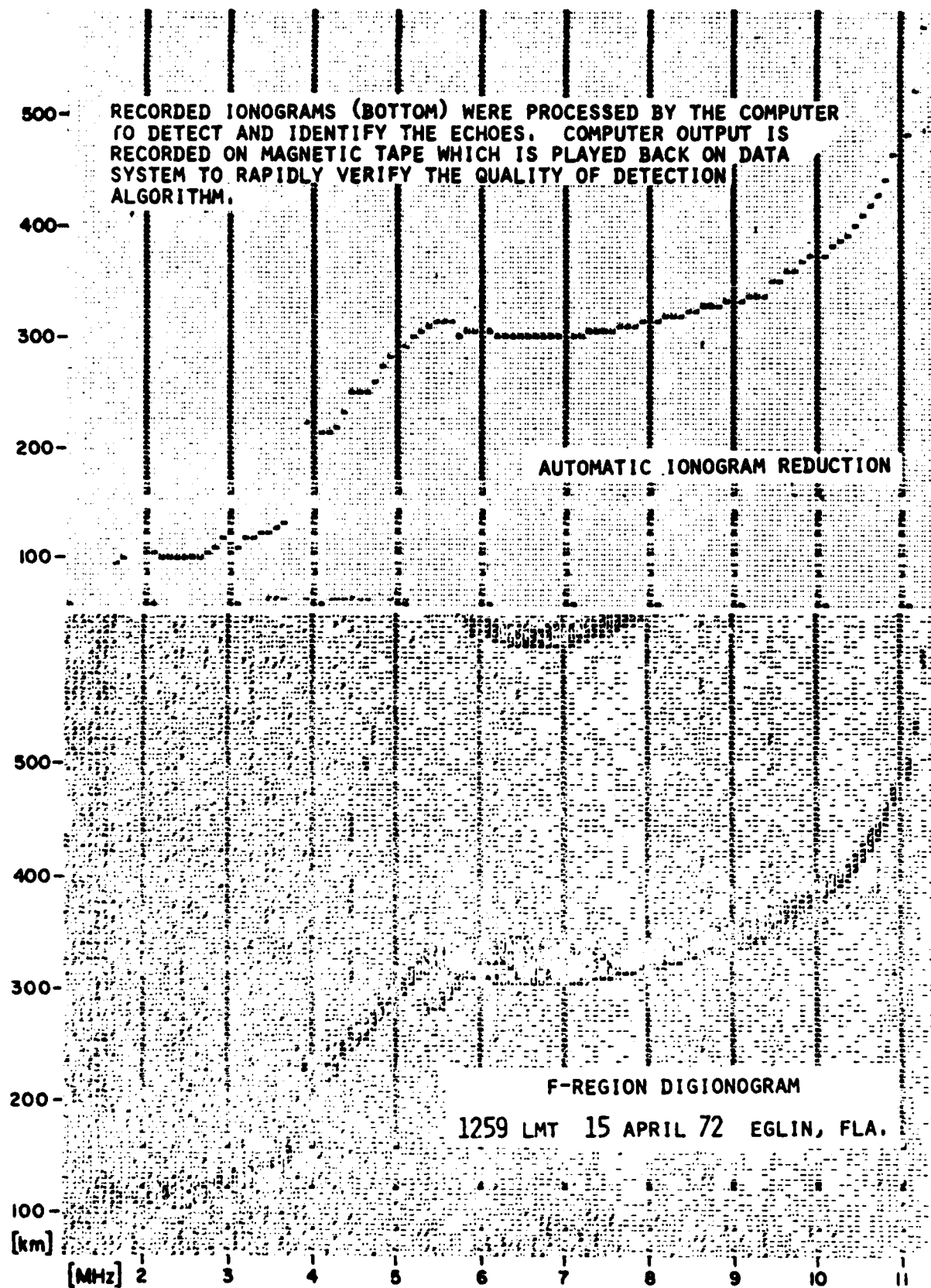


FIGURE 1. AUTOMATIC IONOGRAM SCALING

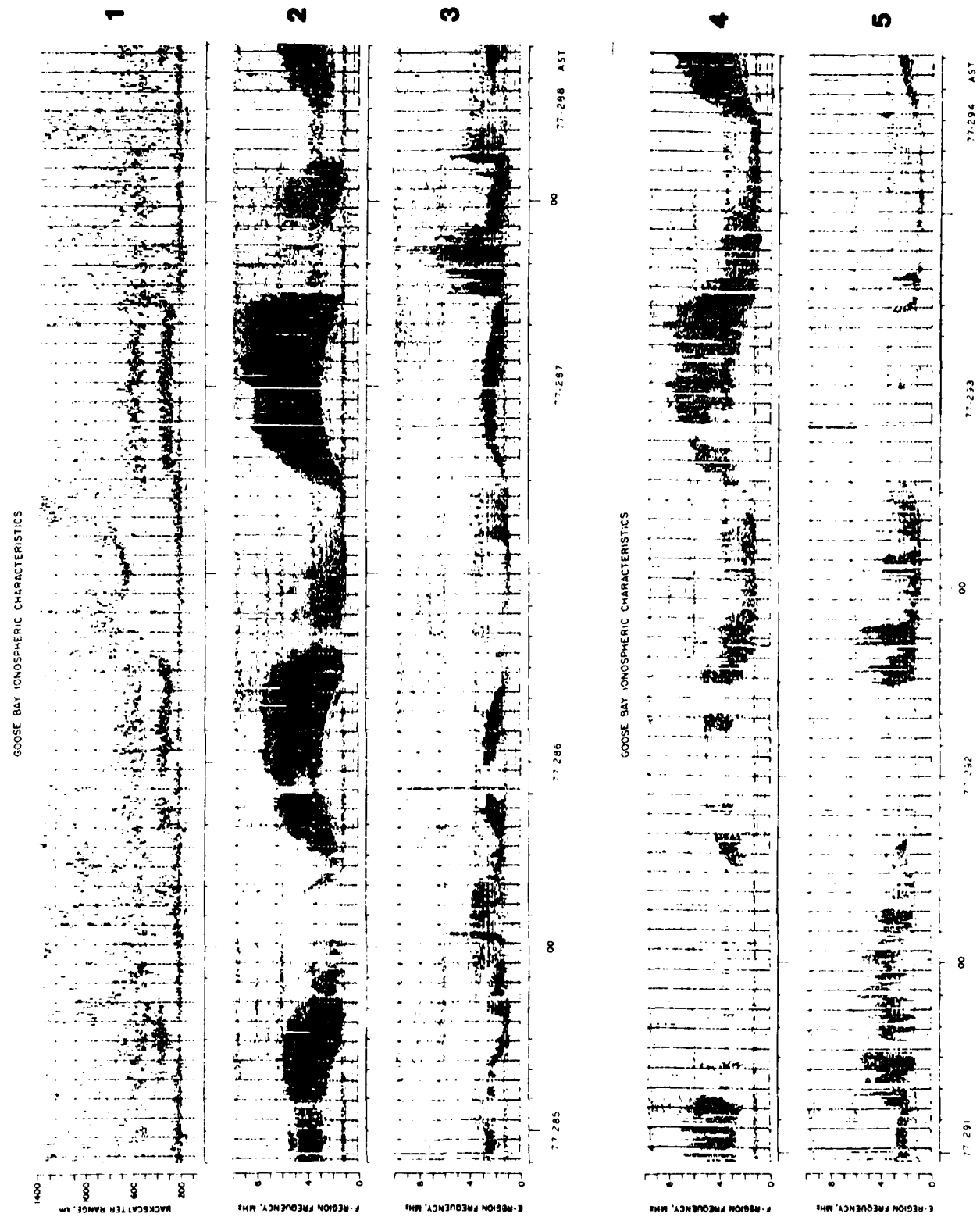
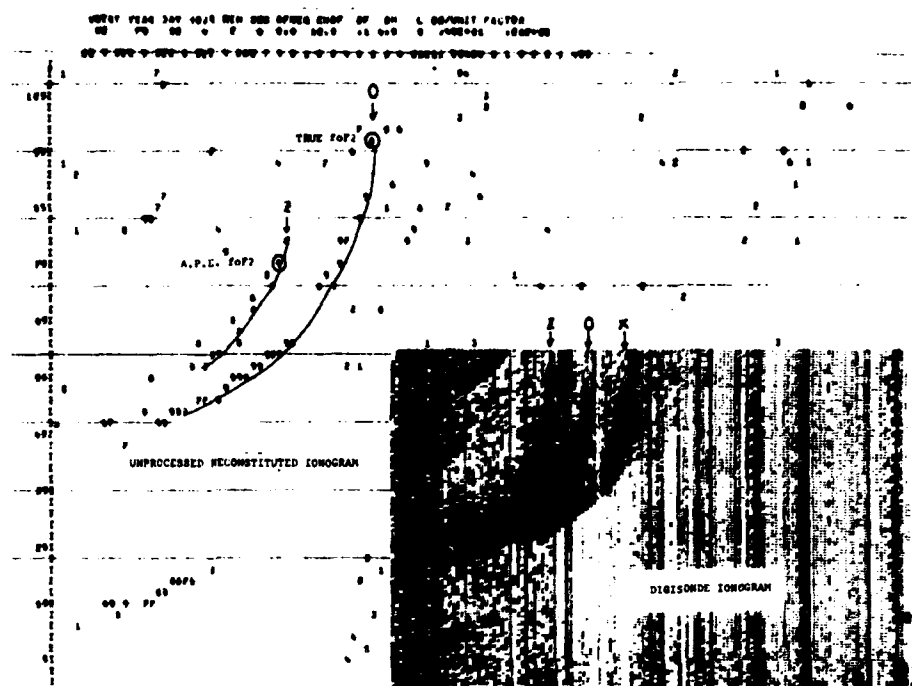
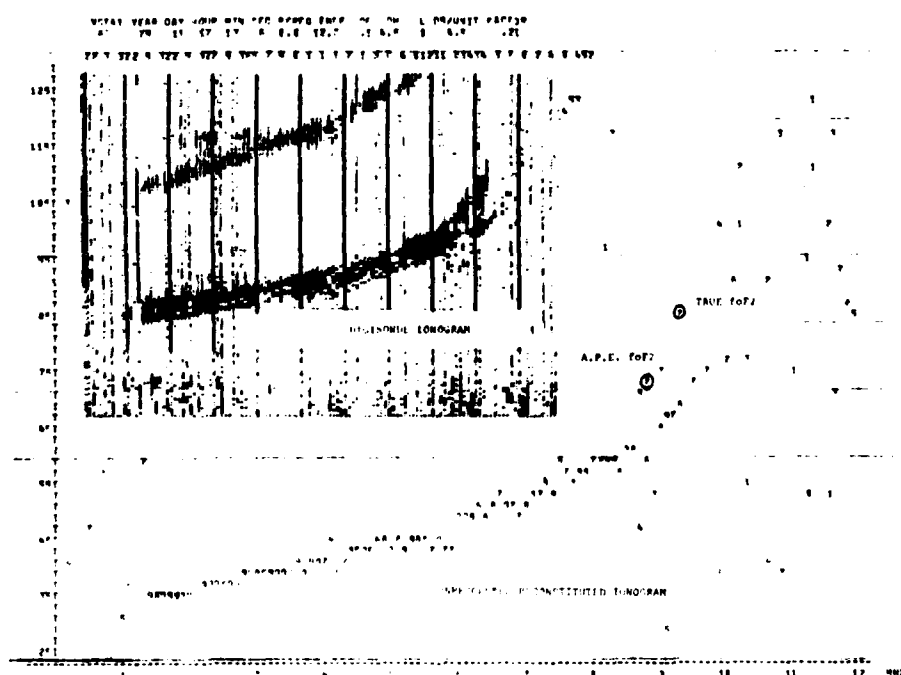


FIGURE 2. IONOSPHERIC CHARACTERISTICS

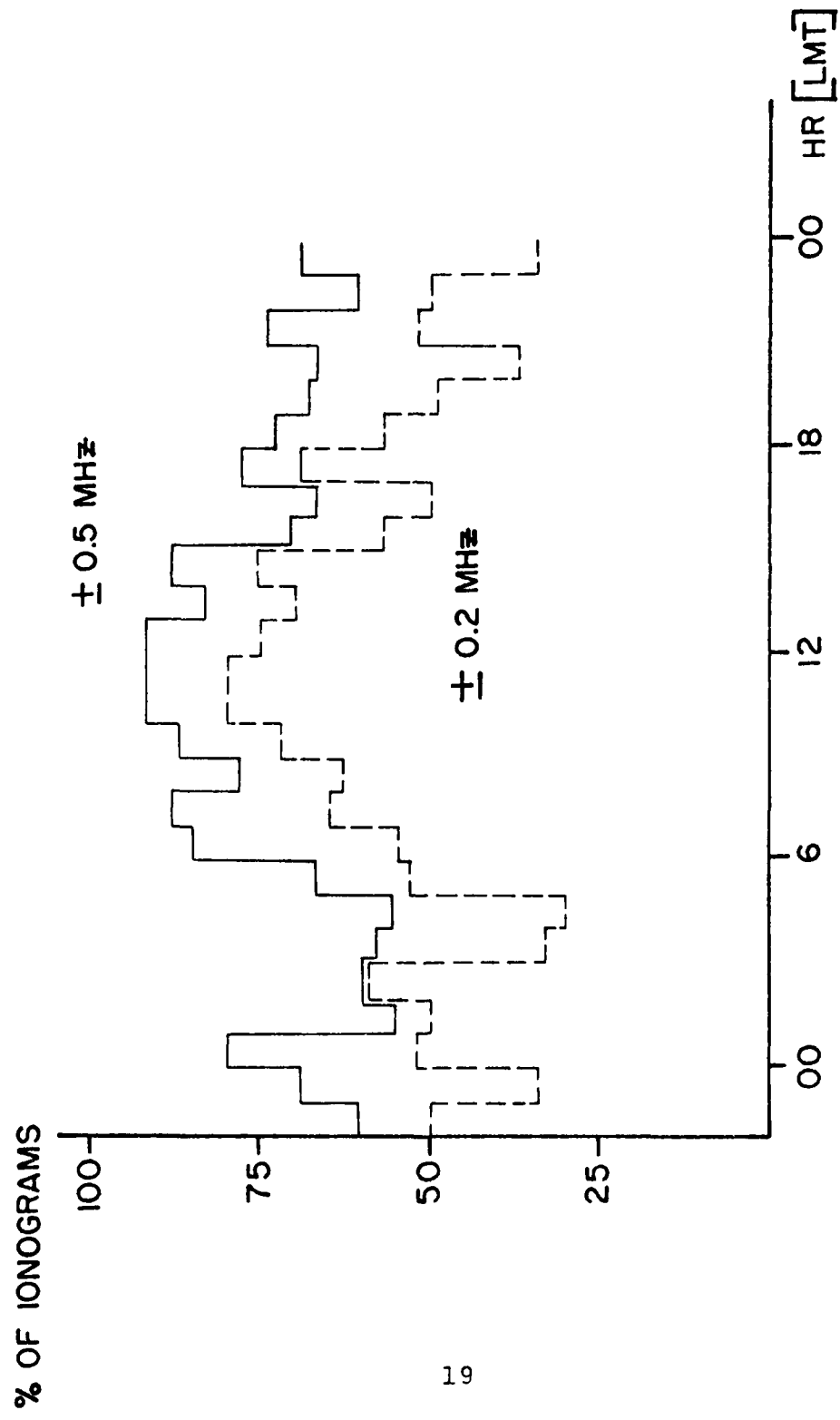


EXAMPLE OF IONOGRAM TO SHOW THE Z COMPONENT



EXAMPLE TO SHOW THE ORDER IN APE IN DETERMINING $\mu_0 F_2$

FIGURE 3



DIURNAL VARIATION OF ERROR (MANUAL f_{oF2} - A.P.E. f_{oF2})

948 IONOGRAMS

5-13 JANUARY 1979

GOCSE BAY, LABRADOR

FIGURE 4

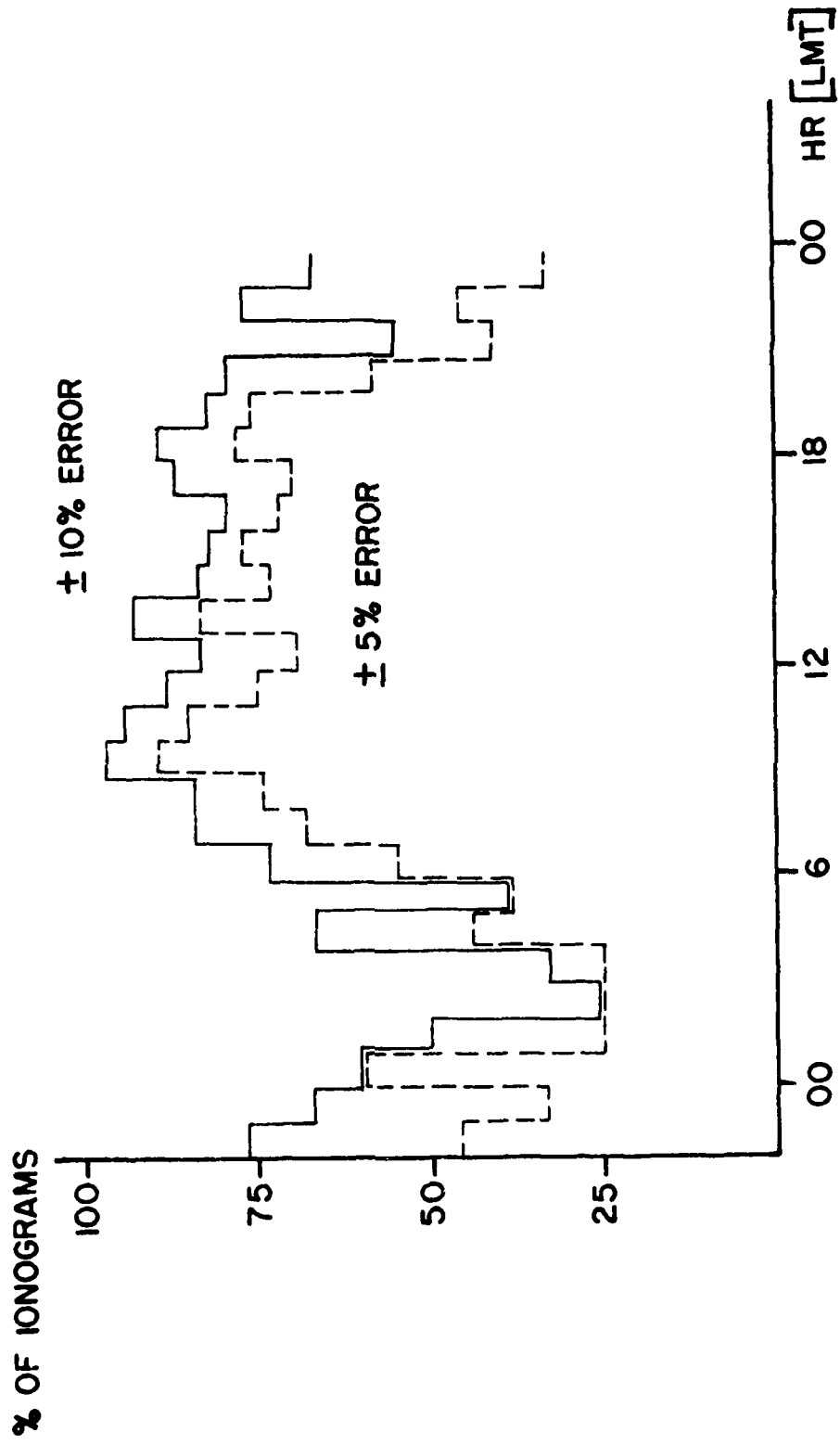


FIGURE 5

DIURNAL VARIATION OF ERROR [MANUAL MUF(3000)-A.P.E. MUF(3000)/MANUAL MUF(3000)]

938 IONOGrams

5-13 JANUARY 1979
GOOSE BAY, LABRADOR

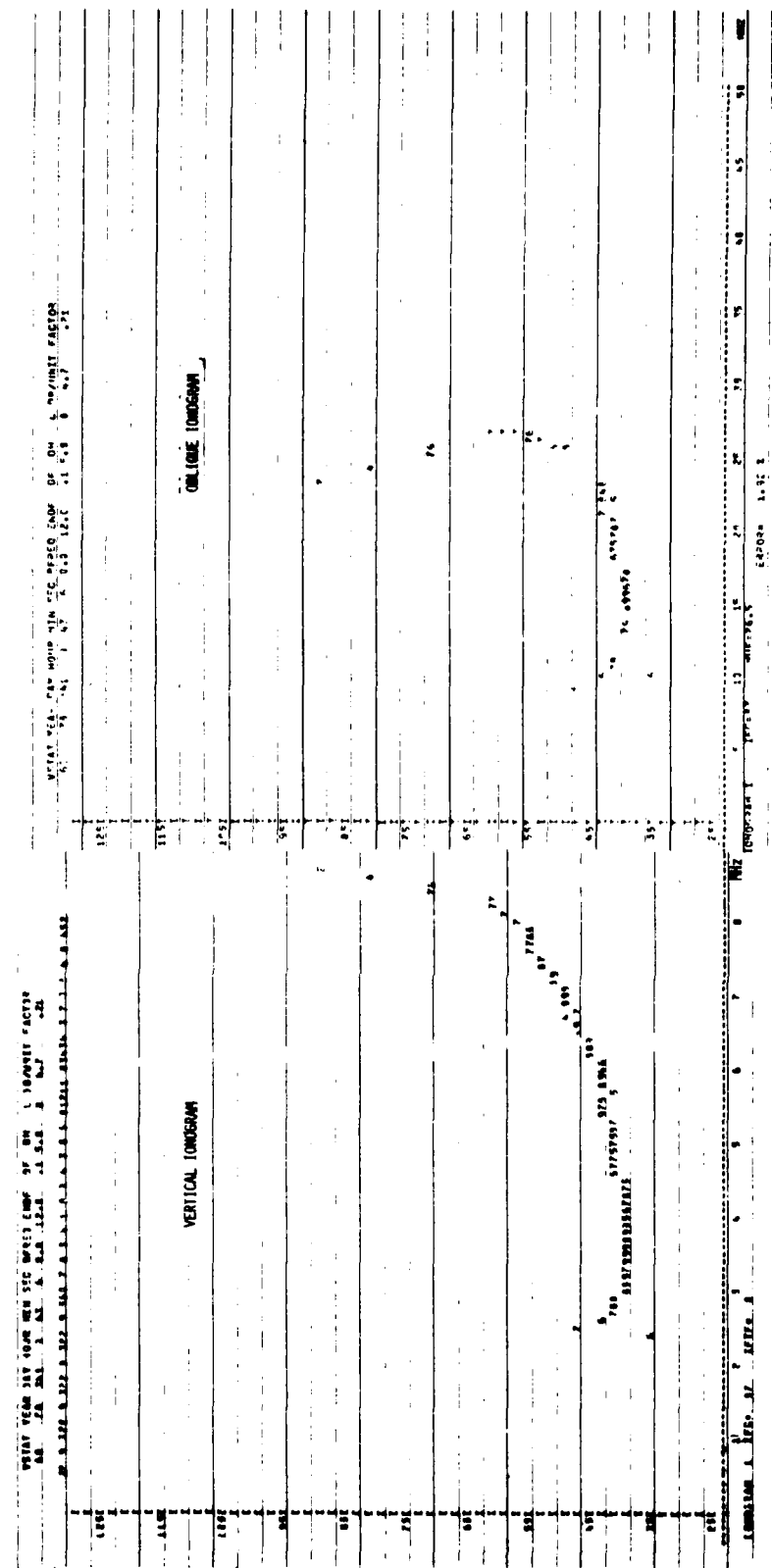


FIGURE 6

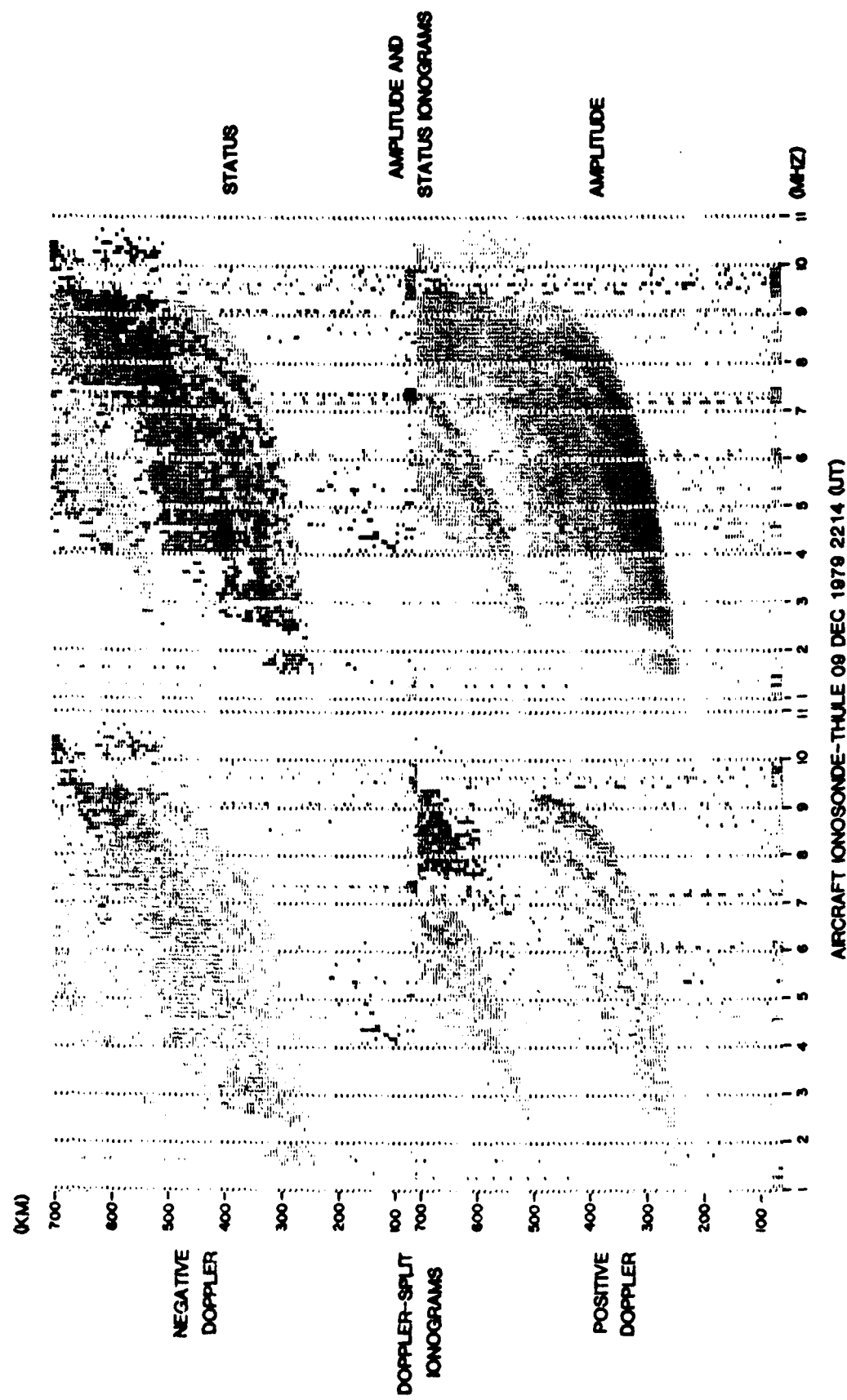
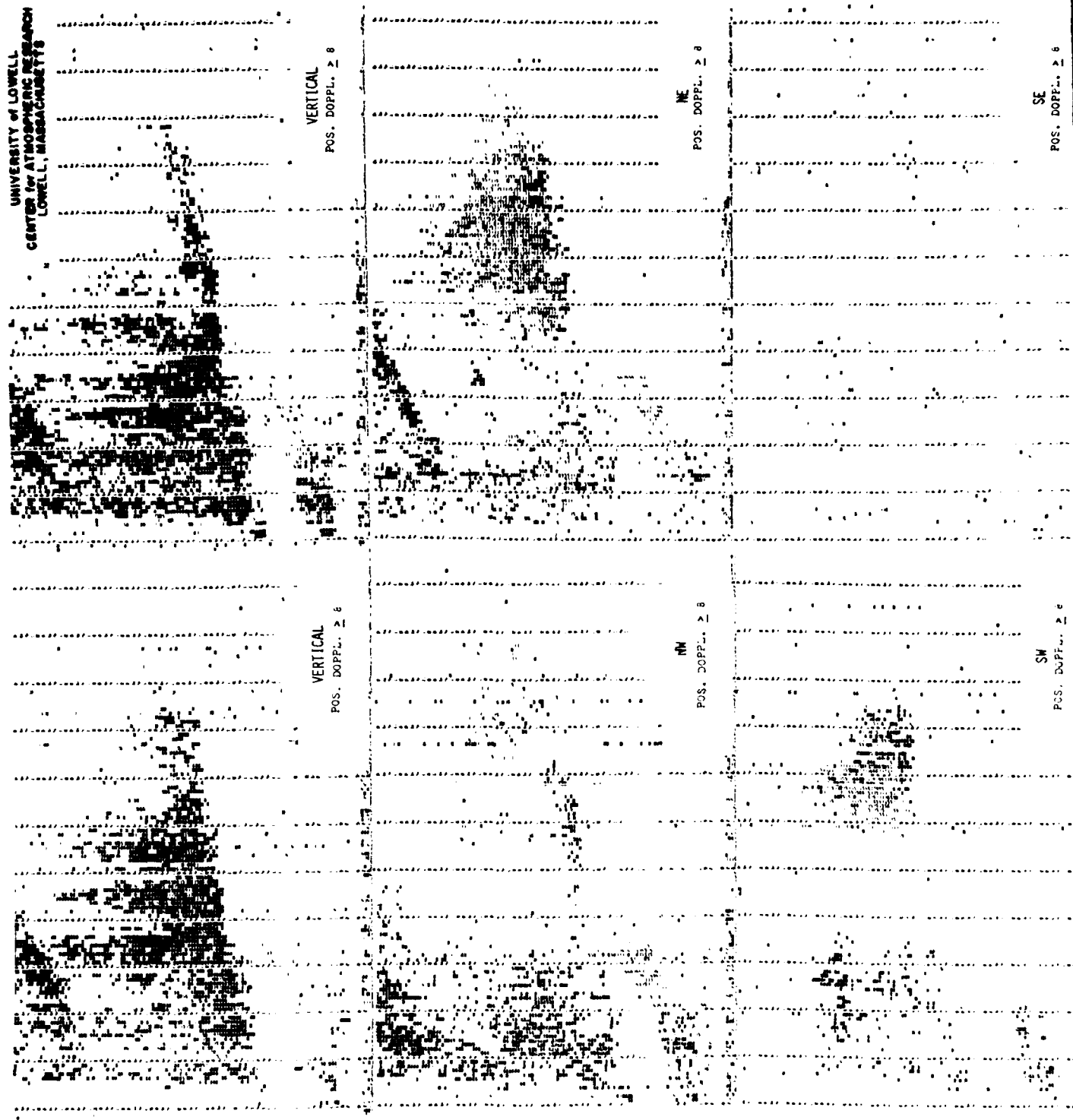


FIGURE 7

KWAJALEIN 21 MARCH 78



DIRECTIONAL IONOGRAMS WITH DOPPLER

FIGURE 8

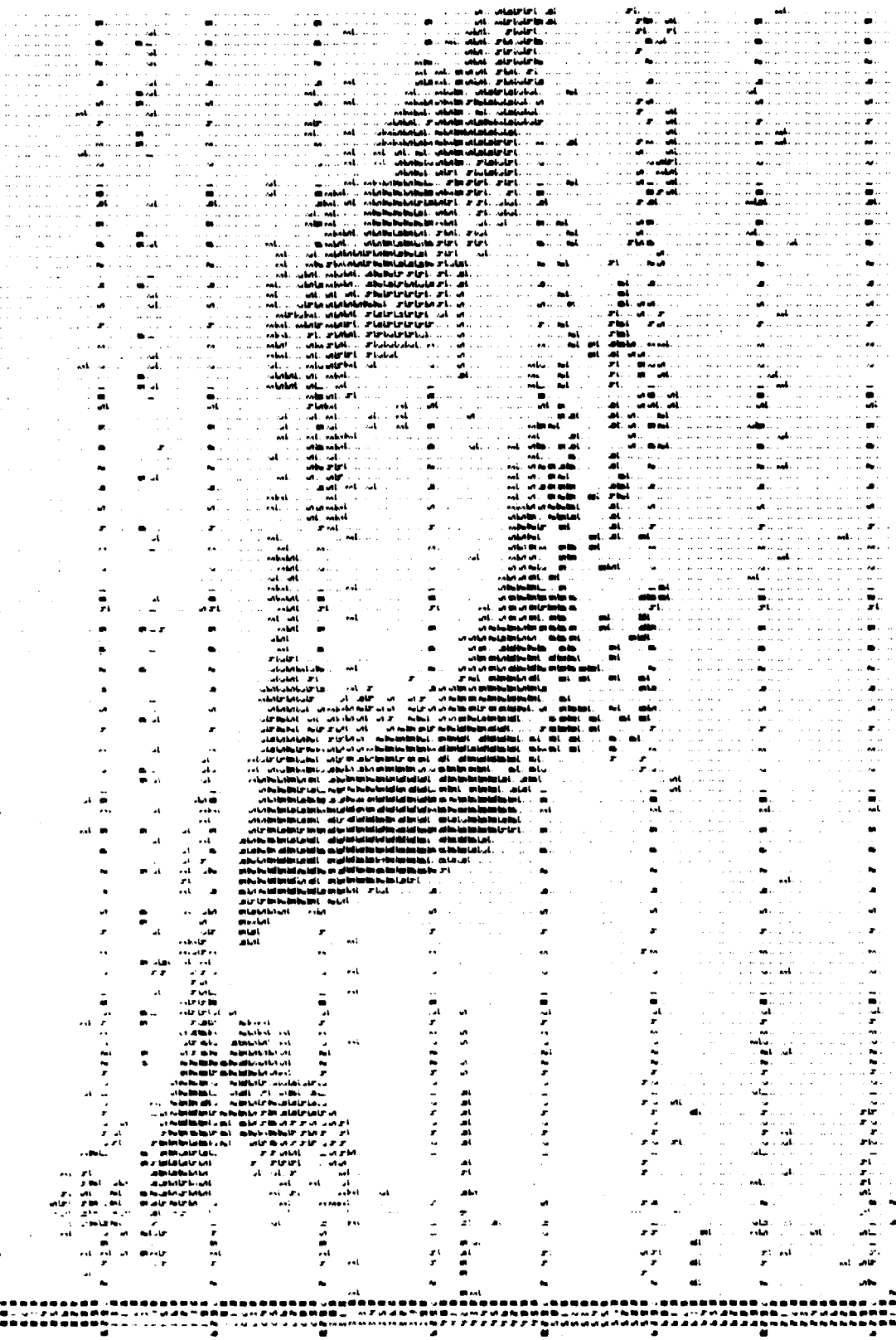


FIGURE 9

4-
DT